Chapter 29
Search for Dark Matter in the Mono−W/$Z(q\bar{q})$ Channel at the ATLAS Experiment

Bibhuti Parida

Abstract We present a search for Dark Matter (DM) particles production in the mono-$W/Z(q\bar{q})$ channel using pp collision data at a centre-of-mass energy of $\sqrt{s}$ = 13 TeV corresponding to an integrated luminosity of 36.1 fb^{-1}, recorded by the ATLAS detector at the Large Hadron Collider (LHC). No significant excess over the Standard Model (SM) prediction is observed. The search results are interpreted in terms of limits on invisible Higgs boson decays into DM particles, constraints on the parameter space of the simplified vector-mediator model and generic upper limits on the visible cross section for W/Z+DM production.

29.1 Introduction

Discovery of DM particles and the understanding of their interactions with SM particles is one of the greatest quests in particle physics and cosmology today. Different experimental approaches are being exploited. The indirect detection experiments search for signs of DM annihilation or decays in outer space whereas the direct detection experiments are related to low-energy recoils of nuclei induced by interactions with DM particles from the galactic halo. The interpretation of these searches is subject to astrophysical uncertainties in DM abundance and composition. Searches at particle colliders, for which these uncertainties are irrelevant, are complementary if DM candidates can be produced in particle collisions. DM signature which can be detected at the LHC experiments is a large overall missing transverse momentum (E_T^{miss}) from a pair of DM particles that recoil against one or more SM particles. Weakly Interacting Massive Particles (WIMPs), one of the leading DM candidates, could be produced in pp collisions at the LHC and detected by measuring the momentum imbalance associated with the recoiling SM particles. So far, several searches for

Bibhuti Parida, On behalf of the ATLAS Collaboration (Speaker), XXIII DAE-BRNS High Energy Physics Symposium, December 10–14, 2018, IIT Madras, India.

B. Parida (✉)
Tomsk State University, Tomsk, Russia
e-mail: bibhuti.parida@cern.ch

P. K. Behera et al. (eds.), *XXIII DAE High Energy Physics Symposium*,
Springer Proceedings in Physics 261,
https://doi.org/10.1007/978-981-33-4408-2_29

DM signatures were performed with LHC pp collision data at centre-of-mass energies of 7, 8 and 13 TeV with no significant deviations from SM predictions observed and set limits on various DM particle models. In this proceedings, we present the latest results of DM particles production in association with a hadronically decaying W or Z boson (mono-W/Z search).

29.2 Search Interpretation and Samples

Two signal models are used to describe DM production in the mono-W/Z final state. These are (i) simplified vector-mediator model, illustrated by the Feynman diagram in Fig. 29.1a, in which a pair of Dirac DM particles is produced via an s-channel exchange of a vector mediator ($Z^{'}$) [1, 2]. There are four free parameters in this model: the DM and the mediator masses (m_{χ} and $m_{Z'}$, respectively), and the mediator couplings to the SM and DM particles (g_{SM} and g_{DM}, respectively) and (ii) invisible Higgs boson decays in which a Higgs boson H produced in SM Higgs boson production processes decays into a pair of DM particles which escape detection as shown in Fig. 29.1b. The free parameter of this model is the branching ratio $B_{H\to \text{inv}}$. The cross sections for different Higgs boson production modes are taken to be given by the SM predictions.

Signal processes within the simplified Z' vector-mediator model are modelled at the Leading Order (LO) accuracy with the MadGraph5_aMCNLO v2.2.2 generator interfaced to the PYTHIA 8.186 and PYTHIA 8.210 parton shower models, respectively. The A14 set of tuned parameters are used together with the NNPDF23lo PDF set for these signal samples. The signal samples within the simplified vector-mediator model are generated in a grid of mediator and DM particle masses, with coupling values set to $g_{SM} = 0.25$ and $g_{DM} = 1$. The mediator mass $m_{Z'}$ and the DM particle mass m_{χ} range from 10 GeV to 10 TeV and from 1 GeV to 1 TeV, respectively. Processes in the mono-W/Z final state involving invisible Higgs boson decays originate from the VH, ggH and VBF SM Higgs boson production mechanisms and were all generated with the POWHEG-BOX v2 generator interfaced to PYTHIA 8.212 for the parton shower, hadronization and the underlying event modelling. The Higgs

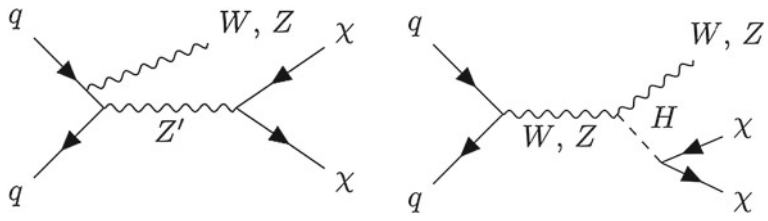

Fig. 29.1 Feynman diagrams for simplified vector-mediator model (left); invisible Higgs boson decay (right)

boson mass in these samples was set to $m_H = 125\,\text{GeV}$ and the Higgs boson was decayed through the $H \to ZZ^\star \to \nu\nu\nu\nu$ process to emulate the decay of the Higgs boson into invisible particles with a branching ratio of $B_{H\to\text{inv}} = 100\%$.

The major sources of background are the production of top-quark pairs ($t\bar{t}$) and the production of W and Z bosons in association with jets (V +jets, where $V = W$ or Z). Other small background contributions include diboson (WW, WZ and ZZ) and single top-quark production. Their contribution is estimated from simulation. Events containing leptonically decaying W or Z bosons with associated jets were simulated using the Sherpa 2.2.1 generator. The NNPDF3.0 Next-to-Next-to-Leading Order (NNLO) PDF set was used in conjunction with dedicated parton shower tuning. For the generation of $t\bar{t}$ events, Powheg-Box v2 was used with the CT10 PDF set in the NLO matrix element calculations. Electroweak t-channel, s-channel and Wt-channel single-top-quark events were generated with Powheg-Box v1. Diboson events with one of the bosons decaying hadronically and the other leptonically were generated with the SHERPA 2.1.1 event generator. The CT10 PDF set was used in conjunction with dedicated parton shower tuning.

29.3 Object Reconstruction and Event Selection

The event selection of this analysis is based on dedicated 1-μ and 2ℓ ($\ell = \mu$ or e) control regions and that relies on the reconstruction and identification of jets, electrons and muons as well as on the reconstruction of the missing transverse momentum ($\text{E}_\text{T}^\text{miss}$). Three types of jets such as '*small-R*' with radius parameter $R = 0.4$, '*large-R*' with radius parameter $R = 1.0$ and '*track jets*' with radius parameter $R = 0.2$ using anti-k_t jet clustering algorithm are employed in this search. The small-R central jets containing b-hadrons are identified using b-tagging algorithm at an operating point with a 70% b-tagging efficiency measured in simulated $t\bar{t}$ events. As for the small-R jets, the track jets containing b-hadrons are identified using the MV2c10 algorithm at a working point with 70% efficiency. Electron candidates are reconstructed from energy clusters in the electromagnetic calorimeter that are associated to an inner detector track. The electron candidates are identified using a likelihood-based procedure in combination with additional track hit requirements. Muon candidates are primarily reconstructed from a combined fit to inner detector hits and muon spectrometer segments. In the middle part of the detector ($|\eta| < 0.1$), where the muon spectrometer coverage is suboptimal, muons are identified by matching a reconstructed inner detector track to calorimeter energy deposits consistent with a minimum ionizing particle. The vector missing transverse momentum, $\text{E}_\text{T}^\text{miss}$, is calculated as the negative vector sum of the transverse momenta of calibrated small-R jets and leptons, together with the tracks which are associated to the primary interaction vertex but not associated to any of these physics objects. A closely related quantity, $\text{E}_\text{T}^\text{miss(no lepton)}$, is calculated in the same way but excluding the reconstructed muons or electrons. The missing transverse momentum is given by the magnitude of these vectors, $\text{E}_\text{T}^\text{miss} = |\text{E}_\text{T}^\text{miss}|$ and $\text{E}_\text{T}^\text{miss(no lepton)} = |\text{E}_\text{T}^\text{miss(no lepton)}|$. In addition, the

track-based missing transverse momentum vector, p_T^{miss}, and similarly $p_T^{miss(no\ lepton)}$, is calculated as the negative vector sum of the transverse momenta of tracks with $p_T > 0.5$ GeV and $|\eta| < 2.5$ originating from the primary vertex. Events studied in this search are accepted by a combination of E_T^{miss} triggers with thresholds between 70 and 110 GeV, depending on the data taking periods with the trigger efficiency is measured using events with large E_T^{miss} accepted by muon triggers.

Two distinct event topologies are considered depending on the Lorentz boost of the vector boson: a merged topology where the decay products of the vector boson are reconstructed as a single large-R jet, and a resolved topology where they are reconstructed as a pair of individual small-R jets. A priority merged selection procedure has been considered, i.e each event is first passed through the merged-topology selection and, if it fails, it is passed through the resolved-topology selection. Thus, there is no overlap of events between the two final state topologies. In the merged (resolved) event topology, at least one large-R jet (at least two small-R jets) and E_T^{miss} values above 250 GeV (above 150 GeV) are required in the final state. The events are again classified according to the number of b-tagged jets present in the events such as with exactly zero ($0b$), one ($1b$) and two ($2b$) b-tagged jets to improve the signal-to-background ratio and the sensitivity to $Z \to b\bar{b}$ decays. Small-R jets (track jets) are used for the b-tagging in the resolved (merged) category. The events in the $0b$ and $1b$ categories with merged topology are further classified into high-purity (HP) and low-purity (LP) regions; the former category consists of events satisfying the p_T-dependent requirements on the jet substructure variable $D_2^{\beta=1}$, allowing an improved discrimination for the jets counting $V \to q\bar{q}$ decays, while the latter one selects all the remaining signal events. Mass window requirements are imposed on the vector boson candidate in the $2b$ tag merged and $0b$, $1b$ and $2b$ tag resolved topologies whereas a W/Z tagger requirement has been applied for the $0b$ and $1b$ tag merged topology. More details of the object reconstruction and event selection used in the analysis can be found in the original published paper [3].

29.4 Background Estimation

The dominant background contribution originates from the $t\bar{t}$ and V+jets production and is estimated by the normalization factors extracted from the Control Regions (CRs). The sub-dominant backgrounds are constraints by theoretical values. The 1-μ CR is designed to distinguish W+jets and $t\bar{t}$ process whereas the 2ℓ CR is designed to estimate the contributions of the Z+jets process selecting $Z \to \mu^+\mu^-$ and e^+e^- decays. More details of the background estimation procedure can be found in [3].

29.5 Systematic Uncertainties

Several experimental and theoretical systematic uncertainties affect the final results of the analysis. Theoretical uncertainties on the signal yield are estimated to be about

10–15% for the simplified vector-mediator model and it is 5–10% for the invisible decays of the Higgs boson. The experimental systematics include large-R jet mass scale and resolution (10% on signal and 5% on background). This is the largest source of experimental systematic uncertainty in the merged topology. The uncertainty in the large-R jet energy resolution is 3% on signal and 1% on background. The uncertainty due to the ${D_2}^{\beta=1}$ substructure parameter is 5–10%. The uncertainties due to the small-R jet energy scale are 6% on signal and 10% on background. The small-R jet resolution uncertainties affect 2–5% and the b-tagging calibration uncertainty affects up to 10%. The uncertainties on the modelling of E_T^{miss} are 1–3% and 2–10% for the background and signal processes, respectively. The uncertainty in the combined 2015 + 2016 integrated luminosity is 2.1%.

29.6 Statistical Interpretation and Results

This search involves 40 analysis regions such as eight zero-lepton signal regions, six one-lepton and six two-lepton control regions, as well as the corresponding sideband regions for each of these twenty categories. A profile likelihood fit [4] is used in the interpretation of the data to search for DM production. The fit variables for different CR and SR are: E_T^{miss} (0ℓ SR), $E_{T,nomu}^{miss}$ (1ℓ CR) and p_T^V (2ℓ CR) respectively. There is a good agreement of data and background prediction in all signal regions. Out of the 40 analysis regions, Fig. 29.2 shows only the signal region distributions of missing transverse momentum, E_T^{miss} with the resolved (left) and merged (right) event topologies after the profile likelihood fit (with $\mu = 0$). The total background contribution before the fit to data is shown as a dotted blue line. The hatched area represents the total background uncertainty. The signal expectations for the simplified vector-mediator model with $m_\chi = 1$ GeV and $m_{Z'} = 600$ GeV (dashed red line) and for the invisible Higgs boson decays (dashed blue line) are shown for comparison. The inset at the bottom of each plot shows the ratio of the data to the total post-fit (dots) and pre-fit (dotted blue line) background expectation.

29.6.1 Limit Calculation

In the search for invisible Higgs boson decays, an observed (expected) upper limit of $0.83(0.58^{+0.23}_{-0.16})$ is obtained at 95% CL on the branching ratio $B_{H\to \text{inv.}}$, assuming the SM production cross sections and combining the contributions from VH, ggH and VBF production modes. The expected limit is a factor of about 1.5 better (while the observed is slightly worse) than the one reached by the previous analysis of Run 1 ATLAS data [5]. In the context of the mono-W/Z simplified vector-mediator signal model, an exclusion limit at 95% CL is calculated on the DM-mediator masses for Dirac DM particles and couplings, $g_{SM} = 0.25$ and $g_{DM} = 1$, which is shown in Fig. 29.3a. For the given coupling choices, vector-mediator masses, $m_{Z'}$, of up to

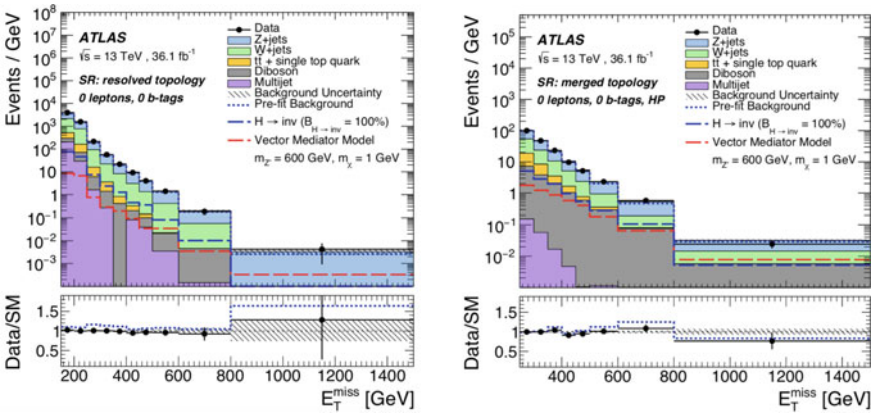

Fig. 29.2 0 *b*-tags resolved event topology (left) and 0 *b*-tags, HP merged event topology (right) [3]

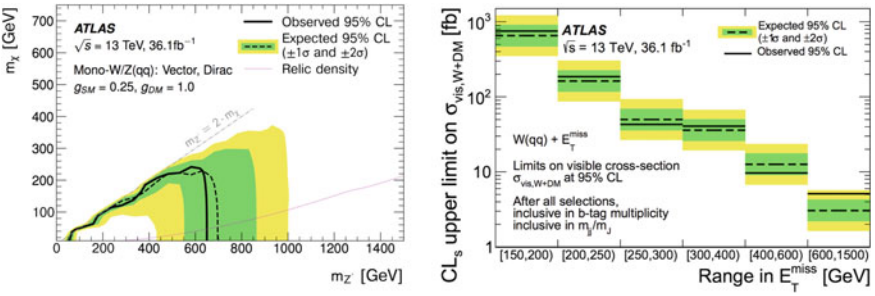

Fig. 29.3 Exclusion limits at 95% CL in the grid of $(m_\chi, m_{Z'})$ (left) and on the visible cross section $\sigma_{\text{vis,W+DM}}$ (right) [3]

650 GeV are excluded at 95% CL for DM masses $m_{\emptyset}$ of up to 250 GeV, agreeing well with the expected exclusion of $m_{Z'}$ values of up to 700 GeV for m_χ of up to 230 GeV. The expected limits are improved by 15–30%, depending on the DM mass, compared to the analysis presented in [6]. In addition to these interpretations, the results are also expressed in terms of generic CL_s upper limits at 95% CL on the allowed visible cross section σ_{vis} of potential W+DM or Z+DM production and is shown in Fig. 29.3b for the W+DM case. The limits on these two processes are evaluated separately to allow more flexibility in terms of possible reinterpretations, as the new models might prefer one of these two final states.

29.7 Summary

A search for DM has been performed in events having a large-R jet or a pair of small-R jets compatible with a hadronic W or Z boson decay, and large E_T^{miss}. It improves on previous searches by virtue of the larger dataset and further optimization of the selection criteria and signal region definitions. The results are in agreement with the SM predictions and are translated into exclusion limits on DM pair production. In the search for invisible Higgs boson decay, an upper limit of 0.83 is observed at 95% CL on the branching ratio $B_{H\to \text{inv.}}$, while the corresponding expected limit is 0.58. Limits are also placed on the visible cross section of the non-SM events with large E_T^{miss} and a W or a Z boson without extra model assumptions.

Acknowledgements The author wants to thank Prof. Dmitri Tsybychev for his valuable comments in the preparation of these proceedings.

References

1. O. Buchmueller, M.J. Dolan, S.A. Malik, C. McCabe, Characterising dark matter searches at colliders and direct detection experiments: vector mediators. JHEP **01**, 037 (2015). arXiv:1407.8257
2. D. Abercrombie et al., Dark Matter Benchmark Models for Early LHC Run-2 Searches: Report of the ATLAS/CMS Dark Matter Forum, arXiv:1507.00966
3. ATLAS Collaboration, Search for dark matter in events with a hadronically decaying vector boson and missing transverse momentum in pp collisions at $\sqrt{s}$= 13 TeV with the ATLAS detector. JHEP **10**(180) (2018). arXiv:1807.11471
4. G. Cowan, K. Cranmer, E. Gross, O. Vitells, Asymptotic formulae for likelihood-based tests of new physics. Eur. Phys. J. C **71** (2011) 1554 [Erratum ibid. C 73 (2013) 2501]. arXiv:1007.1727
5. ATLAS collaboration, Search for invisible decays of the Higgs boson produced in association with a hadronically decaying vector boson in pp collisions at $\sqrt{s}$ = 8 TeV with the ATLAS detector. Eur. Phys. J. C **75**(337) (2015) arXiv:1504.04324
6. ATLAS collaboration, Search for dark matter produced in association with a hadronically decaying vector boson in pp collisions at $\sqrt{s}$ = 13 TeV with the ATLAS detector. Phys. Lett. B **763**(251) (2016) arXiv:1608.02372
7. B. Parida, On behalf of the ATLAS Collaboration, Search for Dark Matter production in association with a hadronically decaying vector boson in pp collisions at $\sqrt{s}$ = 13 TeV with the ATLAS detector, ATL-PHYS-PROC-2018-158, https://cds.cern.ch/record/2647097, PoS(ICHEP2018)787